

Chapter 5

Study of Photoluminescence of GO in both acidic and alkaline Medium: Effect of an Anionic Surfactant (SDS) and a Cationic Surfactant (CTAB)

5.1. Introduction

The availability of several oxygen containing functional groups (epoxy, hydroxyl, carboxyl) on the surface and sheet edges [1-2] and high surface area, GO interacts with many organic, inorganic, biomolecules, polymers [3-5] and surfactants [6-10] to produce several GO based nanomaterials and nanocomposites. Adsorption of surfactants on the GO surface plays an important role for many practical applications in Li-ion battery electrodes [11-12], metal-oxide films [13-14]. Introduction of electrostatic repulsive or steric factors increases the stability of the aqueous GO system [10]. This can be obtained by increasing pH of the medium above pK_a of the carboxylic groups through the utilization of electrostatic repulsion between the negative charges of carboxyl groups on the edges of GO Sheet [15-17]. But when carbon to oxygen ratio is high, pH adjustment is not practically possible. In this situation, stability of the aqueous GO system may be enhanced by using surfactants. The charged head groups of adsorbed ionic surfactants may provide electrostatic repulsion or steric interaction. Considering this fact in mind, the different research groups investigated the stability of GO in aqueous medium in the presence of sodium dodecyl sulphate (SDS) by various methods and also studied the interaction between GO and SDS. Hsieh et al. observed the adsorption behavior of SDS on functionalized graphene sheet (FGS) by conductometric titration [9]. According to them, the surface of FGS is completely covered by monolayer adsorption of 12 μM SDS concentration, when FGS has carbon to oxygen ratio is 18 and they found the critical surface aggregation concentration (CSAC) for surface micelle formation on FGS as 1.5 mM [9]. In another work, related to the stability of FGS in the presence of SDS by optical microscopy and UV-vis study, Aksay and coworkers showed that FGS achieved significant stability in aqueous medium above the monolayer adsorption concentration ($\geq 40 \mu\text{M}$) of SDS [10]. Glover et al. reported the charge driven selective adsorption of SDS on Graphene Oxide by Atomic Force Microscopy and showed that the amount of selective adsorption of SDS depends on the degree of oxidation

[8]. They explained the observed results on the basis of electrostatic repulsion between the negatively charged SDS head groups and the negatively charged hydroxyl groups on oxidized graphene [8]. In this context, it is important to mention that several researchers extensively investigated the adsorption behaviour of surfactants onto graphitic carbons [18-20]. Compared to graphite, adsorption behaviour of SDS on FGS is different. Graphite contains sp^2 hybridized carbon atoms with a high degree of hexagonal order. But, introduction of oxygen containing functional groups in the basal planes of graphene, the overall structure becomes highly disordered due to the presence of defects [21] and so the possibility of the interaction between oxygen containing functional groups and surfactant molecules increases. The self-assembly behaviour of graphene oxide (GO) in the presence of a cationic surfactant (cetyl trimethyl ammonium bromide, CTAB) have been investigated by Xiangyun et al [40]. Vaghri et al. [41] observed intercalation of CTAB between GO layers hindered GO nanosheets aggregation. The interaction occurred between GO and CTAB increases with increasing the amount of CTAB that leads to smaller degrees of oxidation, resulting in fewer defect sites. So, the surfactant intercalation in the interlayer of GO nanosheets, hindered the GO nanosheets aggregation, which may affect the band structure of GO.

Although, there are a number of studies on the interaction of the surfactant with GO in water [6-10], the current literatures do not show much focus on the optical properties and spectral modulation of the GO dispersions in the presence of surfactants. In the present work, we have investigated the effect of an anionic surfactant sodium dodecyl sulphate (SDS) and a cationic surfactant cetyl trimethyl ammonium bromide (CTAB) on the photoluminescence of GO in both acidic and alkaline medium. We have also compared the experimental results with the multi-stage adsorption model given by Aksay and coworkers [9-10] for the interaction of SDS with GO sheets. By studying the photoluminescence of chemically functionalized GO in presence of different concentration of SDS, the critical surface aggregation concentration

(CSAC) for the formation of hemi cylindrical surface micelles on the GO sheets (in the pH \approx 2) has been determined. In addition to this, we have demonstrated the mode of the interaction between GO and surfactants (CTAB, SDS) in acidic and alkaline pH from the view point of the change in the pattern of PL bands. The red edge excitation effect has also been studied to understand the effect of SDS adsorption on GO sheets in acidic pH (\approx 2). This work enlightens the research on the PL of GO in presence of negatively charged surfactants (SDS) and a cationic surfactant (CTAB), which helps to understand the nature of interaction between GO sheets and surfactants (CTAB, SDS) in acidic and alkaline medium. It should be mentioned that, we did not carried out the photoluminescence experiment of GO in alkaline medium in the presence of CTAB due to aggregation formation of GO (i.e. unstable dispersion of GO) resulting from the ionic interaction between the positively charged ammonium ions of CTAB head and the negatively charged carboxyl groups of GO.

5.2. Experimental Section

The different instruments used for this experiment are FT-IR, X-ray diffraction study (XRD) spectrofluorimeter, scanning electron microscopy (SEM) and transmission electron microscopy (TEM), dynamic light scattering (DLS) and TCSPC and details about instrument has been discussed in chapter 3.

5.2.1. Method of Synthesis

The method of synthesis of has been discussed details in chapter 3. In our experimental work, powdered flake graphite was purchased from Sigma-Aldrich. Aniline (Merck) was used without purification. KMnO_4 , NaNO_3 , H_2O_2 , H_2SO_4 (98%), SDS, CTAB were purchased from Merck as analytical pure reagents.

5.3. Result and Discussion

5.3.1. Characterisation

Our synthesised GO has been characterised by different spectroscopic technique such as Raman spectrum, FT-IR spectrum, X-ray diffraction study, scanning electron microscopy (SEM) and transmission electron microscopy (TEM) and has discussed details in chapter 3 with figure. Now, we interpret the characterisation result of our synthesized nanomaterial.

In the Raman spectrum of GO, two Raman peaks at 1350 cm^{-1} and 1596 cm^{-1} , named as D band (disordered band, associated with the reduction in size of the in-plane sp^2 domains) and G band (growth band, due to vibrations of hexagonal lattice, characteristic of graphene-like “honeycomb” structure), respectively are observed. In our GO sample, the Raman spectra [Fig-1(a), Chapter 3] shows the comparable intensity of D band to that of the G peak at $\sim 1596\text{ cm}^{-1}$ and this spectra is a indicates of significant structural disorder due to the harsh oxidation condition in Hummer’s process. The intensity ratio of the D band to G band (I_D/I_G) of our GO is about ~ 1 and this value is very close to the result obtained from GO from Ganguly et al. [24] and Wang et al. [25]. The FT-IR spectrum of GO indicates the presence of C=O groups in the form of free carboxylic acid and hydrogen bonded carboxylic acid moieties by showing two sharp peaks at 1726 and 1622 cm^{-1} respectively, due to the weakening of carbonyl bond in the latter case (Fig. 1b, chapter 3). A broad band having a center at $\sim 3380\text{ cm}^{-1}$ is appeared mainly due to the stretching mode of vibration of the -OH functional group, which indicates that GO contains the numerous surface hydroxyl groups (-OH group). In the XRD spectrum of GO [Fig. 1c, chapter 3] shows a most intense sharp diffraction peak at $2\theta = 7.97^\circ$ corresponds to the (001) diffraction plane with an interlayer spacing of 1.11 nm [26]. The larger interlayer distance of GO from natural graphite flake might be due to the formation of hydroxyl, epoxy and carboxyl like oxygen-containing functional groups [26]. Another low intense peak appeared at $2\theta = 25.97^\circ$, this value is slightly lower than natural graphite flake which is due the the reflection of

(002) plane [27]. The SEM images of GO displayed an exfoliated layer of several micrometers with a curled morphology [Fig. 1(d), 1(e), 1(f), 1(g) in chapter 3].

5.3.2. Absorption Spectra

UV-Vis absorption spectrum of aqueous dispersion GO in acidic ($\text{pH} \approx 2$) and alkaline ($\text{pH} \approx 10$) does not exhibit any distinct band structure in the presence and absence of both surfactant CTAB and SDS, only broad spectral features are found [(Fig. 1(a), Fig. 1(b) and Fig. 1(c)]. Absorption of the aqueous dispersion of GO below 250 nm may be assigned to π - π^* transition of C=C and whereas absorption at higher wavelength may be due to n- π^* transition of C=O bond [28-29]. The absorption spectral pattern of aqueous GO dispersion remain unchanged in the presence of both surfactant CTAB and SDS.

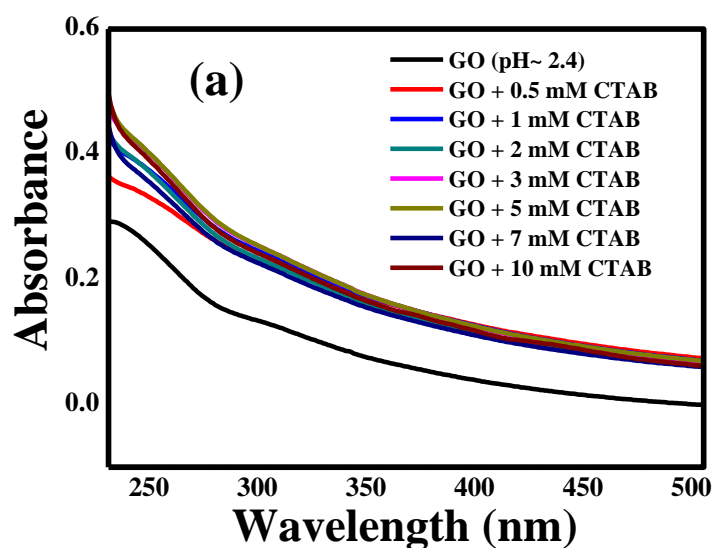


Fig. 1 (a) Absorption spectra of GO dispersion with different CTAB concentration at $\text{pH} \approx 2$

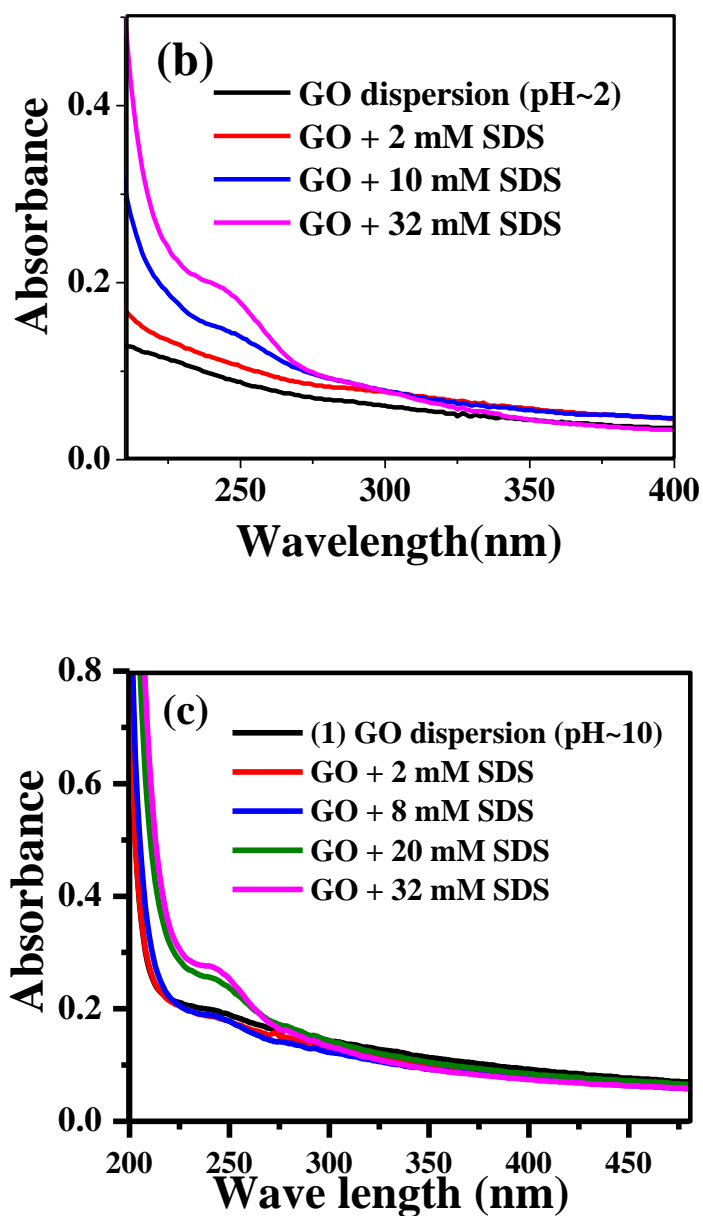


Fig. 1 Absorption spectra of GO dispersion with different SDS concentration at (b) pH \approx 2 (c) pH \approx 10

5.3.3. Photoluminescence of GO

Due to the intrinsic inhomogeneity of GO material, the fluorescence spectra of GO dispersion show interesting features dependent upon the excitation wavelength and pH [30]. We extensively studied the emission characteristics of GO dispersion by exciting the sample at 240 nm (π - π^* band) and at 280 nm (n - π^* band), by varying concentration of surfactants (SDS, CTAB) in both acidic and alkaline medium. Although the photoluminescence property of GO depends on the layer number, estimation of layer number is not possible by the spectroscopic data.

In acidic medium ($\text{pH} \approx 2$), when the aqueous dispersion of GO is excited at 240 nm, an emission band is appeared at 390 nm (Fig. 2a) as obtained by Dutta et al. [30]. Addition of SDS up to 32 mM to the aqueous GO dispersion, a 36 nm blue shift of the emission band is observed (Fig. 2a). Similarly, exciting the aqueous dispersion of GO ($\text{pH} \approx 2$) at 280 nm, the emission band is obtained at 366 nm and a blue shift of 33 nm is found in the presence of 32 mM SDS concentration (Fig. 2b). For the both excitation wavelength at 240 nm and 280 nm, we have found the blue shift of the emission band in two stages. Exciting at 240 nm, first stage blue shift is observed from 390 nm to 368 nm if the concentration of SDS is greater than 2 mM and this emission band is unchanged up to 12 mM SDS. Further blue shift from 368 nm to 354 nm is obtained when the concentration of SDS is above 12 mM (Fig. 3a). Similarly, exciting the acidic dispersion of GO at 280 nm, first blue shift is observed from 366 nm to 344 nm, for the concentration of SDS greater than 2 mM and above 12 mM concentration of SDS, further blue shift is obtained from 344 nm to 333 nm (Fig. 3b). For both the cases above 12 mM SDS concentration, there is no further shift in the emission maxima as the surfaces of GO is almost fully covered by the SDS. Similarly, exciting the aqueous dispersion of GO ($\text{pH} \approx 2$), both at 240 nm and at 280 nm in the presence of 10 mM CTAB, a 38 nm blue shift of the emission maxima is observed.[Fig. 4a and Fig. 4b]

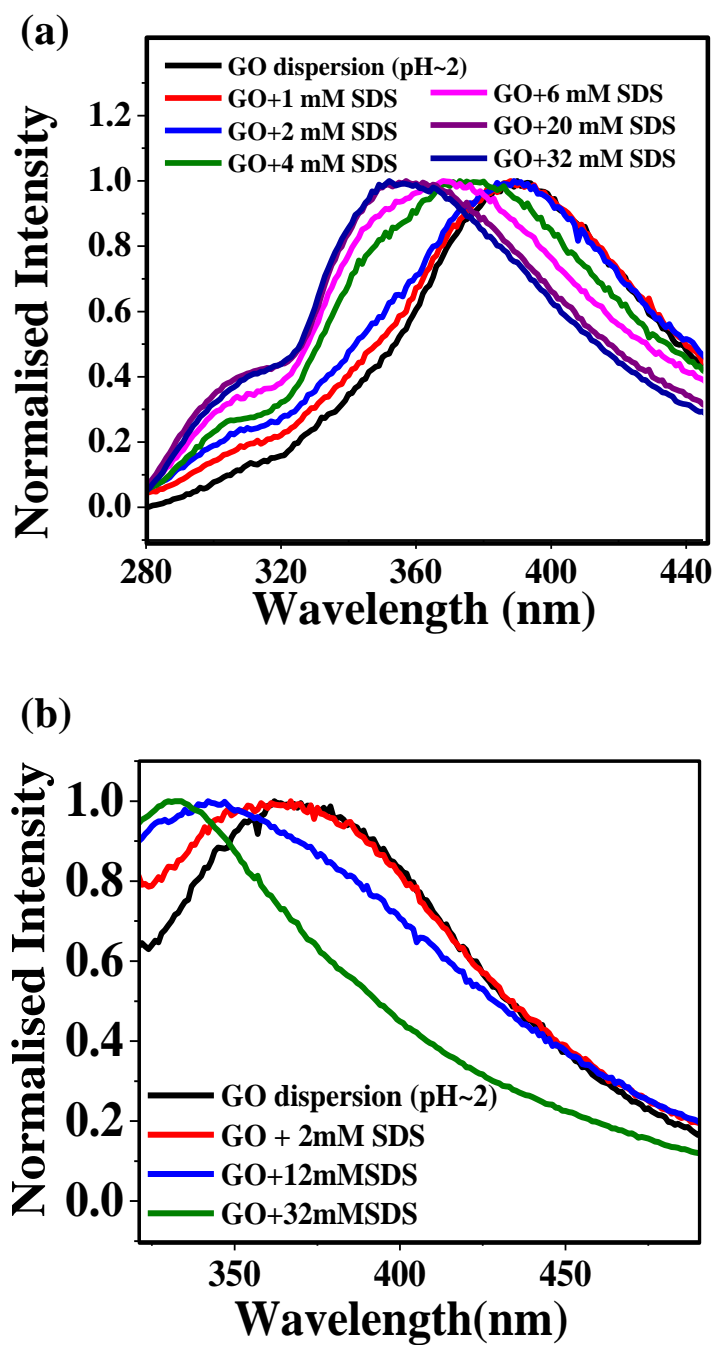


Fig. 2 Photoluminescence Spectra of acidic dispersion of GO with different SDS concentration

(a) $\lambda_{\text{ex}} = 240 \text{ nm}$ (b) $\lambda_{\text{ex}} = 280 \text{ nm}$

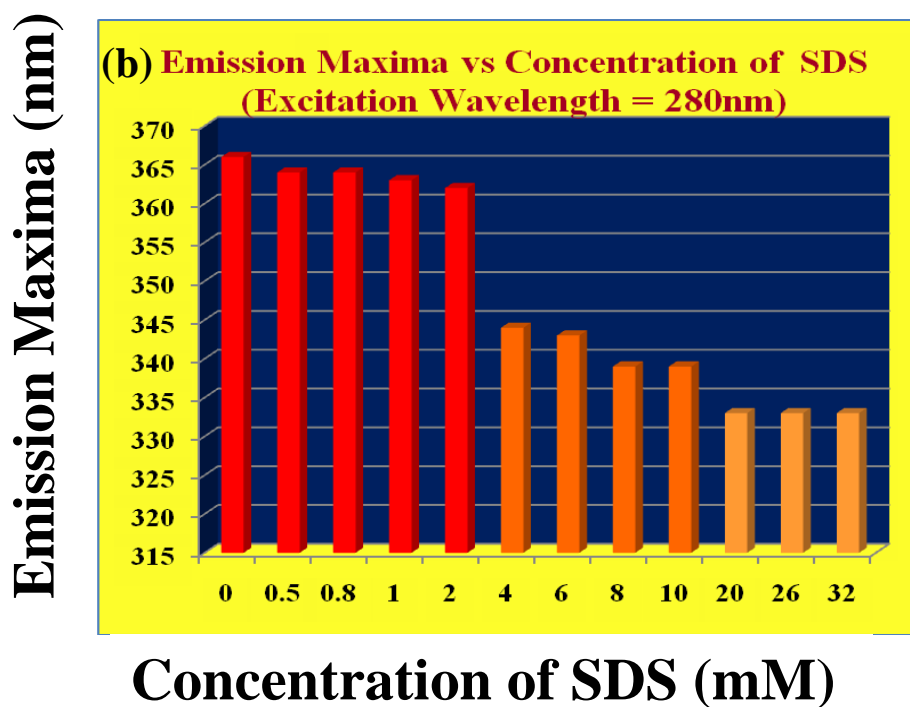
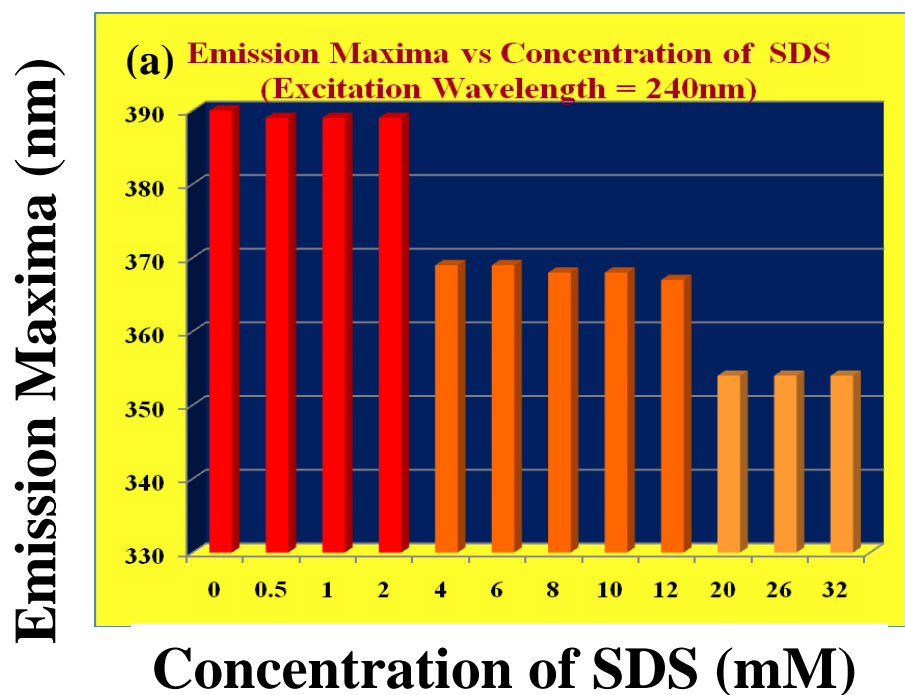


Fig. 3 Plot of Emission Maxima (nm) against concentration of SDS

(a) $\lambda_{ex} = 240 \text{ nm}$ (b) $\lambda_{ex} = 280 \text{ nm}$

This two stage blue shift of the emission maxima of GO (pH~2) in the presence of SDS may be due to the nonpolar environment around the fluorophoric moiety, resulting from the adsorption of SDS on GO surface. Above 2 mM concentration of SDS, monolayer adsorption of SDS on the GO sheets has been taken place and so our photoluminescence study confirms that critical surface aggregation constant (CSAC) is greater than 2 mM which is very close to the observation of Hsieh et al. [9,10]. Above 12 mM SDS concentration, hemi spherical surface micelles are formed on the GO surface resulting a highly non polar environment around the fluorophoric moiety. The blue shift of emission maxima of GO in the acidic medium in the presence of CTAB may also due to creation of nonpolar environment by the formation of hemispherical surface micelle. The ionic interaction between the positively charged ammonium ions of CTAB head and the negatively charged surface charge of GO leads to form hemispherical micelle. The zeta potential values of aqueous GO dispersion [31] at various pH indicates GO contains negative surface charges [17] arising from the carboxylate groups at the edges and the negative surface charge of GO increases with increase in pH. So, the ionic interaction become stronger between GO and CTAB in the alkaline medium, that leads to form aggregate of GO (i.e. unstable dispersion of GO). Thus, we did not carried out the photoluminescence experiment of GO in alkaline medium in the presence of CTAB.

Here, another important observation needs to mention that a small but distinct shoulder is appeared at around 305 nm ($\lambda_{ex} = 240$ nm) in case of the acidic dispersion of GO with SDS concentration greater or equal to 4 mM (Fig. 2a). The emission band at 305 nm also appeared ($\lambda_{ex} = 240$ nm) in the presence of CTAB of concentration greater or equal to 2 mM [Fig. 4a]. To explore the origin of this band we have to consider the extent of π - π stacking interaction between two adjacent GO sheets which will be discussed in details after presenting the luminescence features in alkaline medium.

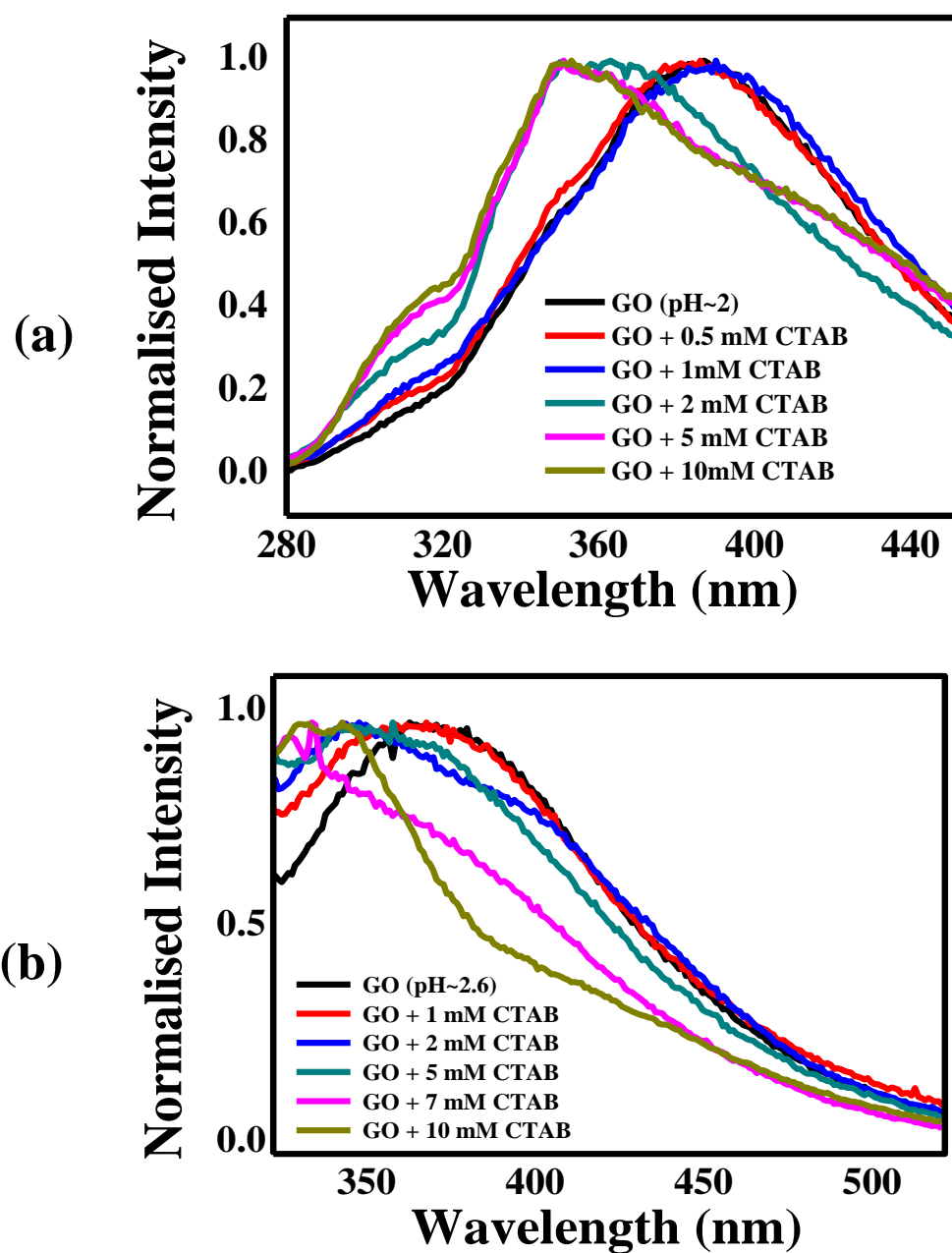


Fig. 4 Photoluminescence Spectra of acidic dispersion of GO with different CTAB concentration

(a) $\lambda_{\text{ex}} = 240 \text{ nm}$ (b) $\lambda_{\text{ex}} = 280 \text{ nm}$

The exhibition of a marked blue shift because of nonpolar environment surrounding the fluorophoric moiety of GO as a result of the adsorption of SDS may be originated from the restricted motion of the solvent molecules (water) by various non-covalent type interactions, H-bonding etc. Solvent relaxation time is usually very much lower than the fluorescence life time of traditional fluorophores [32]. Thus, the solvent relaxation becomes complete before the fluorescence emission and so a red shifted emission from an equilibrium state is observed. Whereas, in the case of slow solvent relaxation time compared to fluorescence life time results a time dependent red shift. Conventionally this time dependent fluorescence Stokes shift (TDFSS) is studied through the construction of time resolved emission spectra (TRES) by monitoring the wavelength dependent fluorescence decay where a growth followed by decay is observed. But, the temporal resolution of our instrumental set up (a pulse width of 600 ps) makes us unable to construct TRES for this study. Again, due to this slow solvent relaxation, a common phenomenon namely, Red Edge Effect (REE) is observed as the rate of change in emission energy due to solvation is higher in magnitude with respect to the life time of the fluorophore. This leads to continuous shift of emission peaks originated from the excitation at gradually increasing wavelengths at the red end of the absorption spectrum. Recently, these types of REE for strongly alkali treated GO were reported by Wu and coworkers [33,34]. Although, excitation dependent emission could come from various functional groups present in GO, gradual red shift in the emission band by the increase in the excitation wavelength at the red end of the absorption spectrum, is not observed for the aqueous dispersion of GO. Only in the presence of high concentration of SDS, such observation is obtained. So, the observation of REE due the presence of various fluorophores within GO may be ruled out.

Considering this fact in mind, we have studied the REE for the aqueous dispersion of GO (pH \approx 2) in the presence of 32 mM SDS. Exciting the aqueous dispersion of GO (pH \approx 2) in the presence of 32 mM SDS at the red end of the absorption spectra (at 360 nm and above),

a gradual shift in the emission maxima was observed (Fig. 5a). This observation clearly suggests that adsorption of the SDS as hemispherical micelles on the GO sheets slows down the solvent relaxation either by shielding the fluorophoric moiety from the solvent dipoles or by introducing confinement on the motion of solvent dipoles through some soft non covalent binding. This leads to the longer time scale of the stabilization of excited state's energy solvation process compared to the life time of the fluorophoric moiety of GO. The plot of emission maxima against excitation wavelength was obtained as linear (Fig. 5b). This indicates that the change in emission maxima ($\Delta\lambda_{em}$) is independent of the excitation wavelengths at the red end of the absorption band.

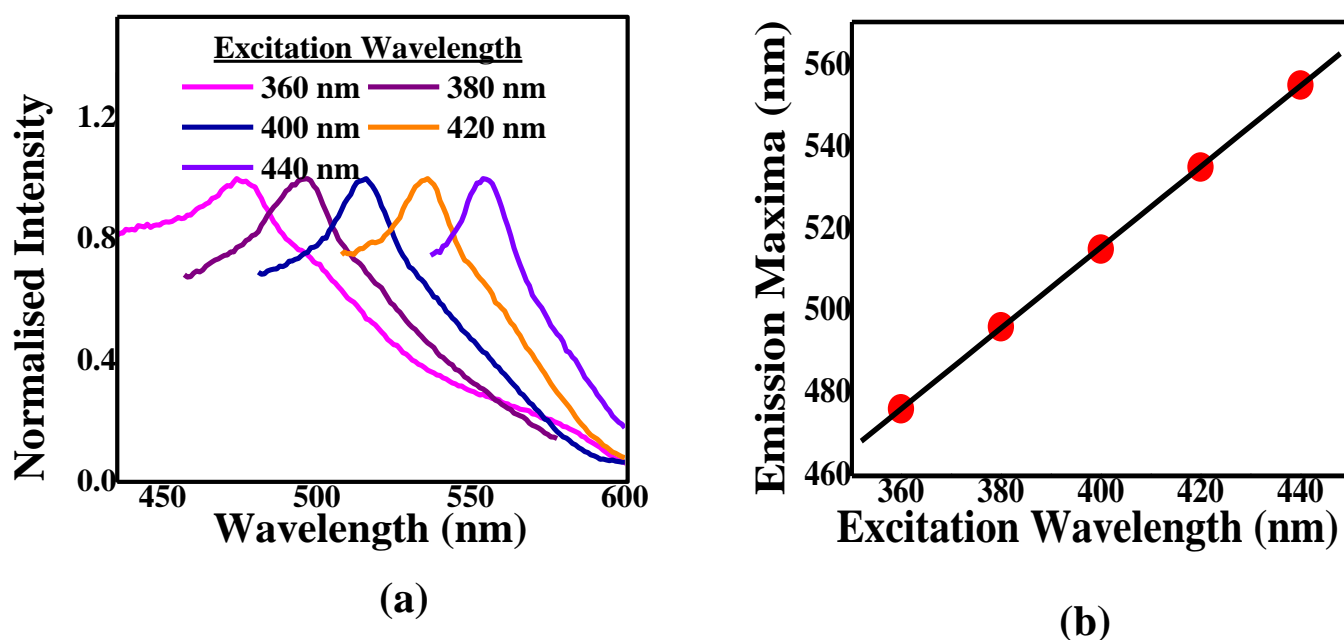


Fig. 5 (a) Plot of photoluminescence spectra at the different excitation wavelength at the red end of the absorption spectra of 32 mM SDS added GO dispersion (b) Plot of Emission Maxima vs excitation wavelength of 32 mM SDS added GO dispersion

We have also studied the photoluminescence of aqueous dispersion GO in alkaline medium of $\text{pH} \approx 10$. When the aqueous dispersion GO of $\text{pH} \approx 10$ was excited at the wavelength 240 nm, the emission band appeared at 347 nm (Fig. 6a). The fluorescence peak of the aqueous dispersion GO is shifted from 390 nm to 347 nm by changing the pH of the medium from 2 to 10 is due to increase in interlayer spacing of GO resulting from the repulsion between negatively charged carboxylic acid functional groups at the edge of GO sheets [30]. Apart from this, a small but distinct shoulder around 303 nm is observed in the alkaline medium (Fig. 6a) and this type of low intense PL band may be appeared due to the benzoic acid or phenol like structure [35,36]. But, in the presence SDS, intensity of the emission band at 303 nm is increased. These types of emission patterns remain same up to 32 mM SDS. To interpret the enhancement of the intensity of the photoluminescence band at 303 nm, we have to consider the mode of interaction between GO and SDS at highly alkaline pH. The zeta potential values of aqueous GO dispersion [31] at various pH indicates GO contains negative surface charges [17] arising from the carboxylate groups at the edges. Hence, SDS adsorption on the GO sheet is hindered due to repulsion between negative head groups of SDS and negatively charged carboxylate groups. But, surfactants may be intercalated between GO layer [7] and this intercalation disrupts the π - π stacking interaction within successive GO sheets, Song et al. reported the intercalation of anionic surfactant to increase the dispersion stability of functionalized graphene [37]. However, the disruption of π - π stacking interaction because of the intercalation SDS within the basal plane of GO may lead to largely separated GO layers. With the increase in the distance between basal planes of GO, the band gap of GO moiety increases [30]. Increase in intensity of the blue shifted band at 303 nm may be due to the increase in the band gap of GO and also due to the pronounced effect of the PL band of the benzoic acid or phenol like moiety present in the GO sheets.

Fig. 6

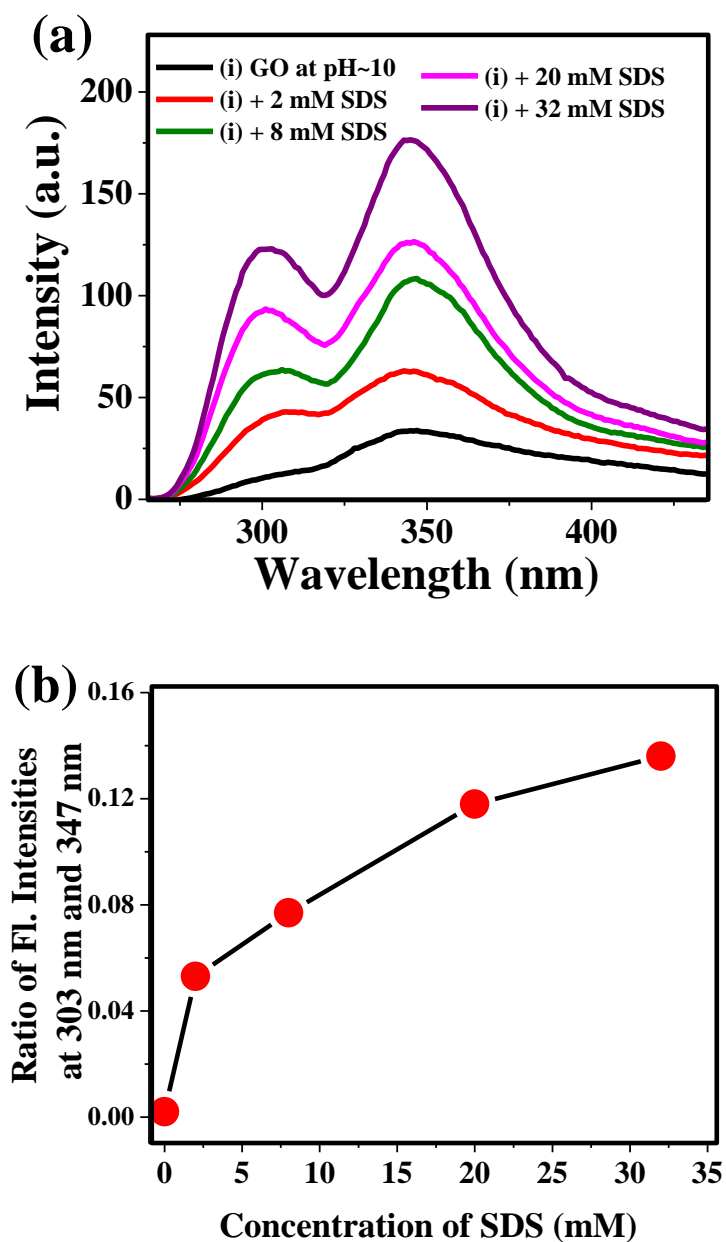


Fig. 6 (a) Photoluminescence Spectra of alkaline dispersion of GO (pH ≈ 10) with different SDS concentration ($\lambda_{\text{ex}} = 240 \text{ nm}$) (b) Plot of ratio of fluorescence intensities at 303 nm and 347 nm vs concentration of SDS

Plot of ratio intensities at 303 nm and 347 nm of alkaline dispersion of GO against SDS concentration (Fig. 6b) shows that with increase in SDS concentration photoluminescence intensity at 303 nm is enhanced as a result of weakening of π - π stacking interaction due to increase in the extent of SDS intercalation within GO layers and this leads to the observation of more prominent emission from benzoic acid or phenol like moiety as the interaction between the two successive GO layers is negligibly small in the presence of SDS. On the basis of this discussion, the appearance of small shoulder at 303 nm in the luminescence spectra (Fig. 2a) of acidic dispersion of GO in the presence of SDS (concentration ≥ 4 mM) is interpreted as a consequence of very weak π - π interaction due to the intercalation of SDS between GO layers. Similarly, the emission band at 305 nm also appeared ($\lambda_{\text{ex}} = 240$ nm) in the presence of CTAB of concentration greater or equal to 2 mM [Fig. 4a], which is due to very weak π - π interaction due to the intercalation of CTAB between GO layers. Onyang and coworkers indicated the presence of long wavelength excimer photoluminescence band due to π - π overlapping between successive GO sheets and another blue shifted photoluminescence band of monomeric GO species without interlayer π - π interaction at very low concentration of GO [38]. Similar type of observation was also found for polyaromatic compounds [39]. Then, the blue shifted fluorescence band at 303 nm is due the GO fluorophoric moieties with widely separated basal planes resulting very high band gap. But, further investigation using the time resolved study is required to confirm this type of phenomenon.

5.3.4. Comparative Photoluminescence

The effect of both an anionic surfactant (SDS) and a cationic surfactant (CTAB) on the photoluminescence spectra of GO in acidic ($\text{pH} \approx 2$) and alkaline ($\text{pH} \approx 2$) dispersions may be summarized by Fig. 7. It should be mentioned that, we did not carried out the photoluminescence experiment of GO in alkaline medium in the presence of CTAB due to aggregation formation of GO (i.e. unstable dispersion of GO) resulting from the ionic

interaction between the positively charged ammonium ions of CTAB head and the negatively charged carboxyl groups of GO. In acidic dispersion, addition of SDS results a marked blue shift from 390 nm to 354 nm obtained by exciting the GO dispersion at 240 nm which may be explained by the formation of hemispherical SDS micelles on the GO sheets resulting a non polar environment and restriction of the movement of the solvent (water) molecules (Fig. 8a). The 38 nm blue shift of emission maxima of GO in the acidic medium in the presence of CTAB may also due to creation of nonpolar environment by the formation of hemispherical surface micelle. The ionic interaction between the positively charged ammonium ions of CTAB head and the negatively charged surfaced charged of GO leads to form hemispherical surface micelle.

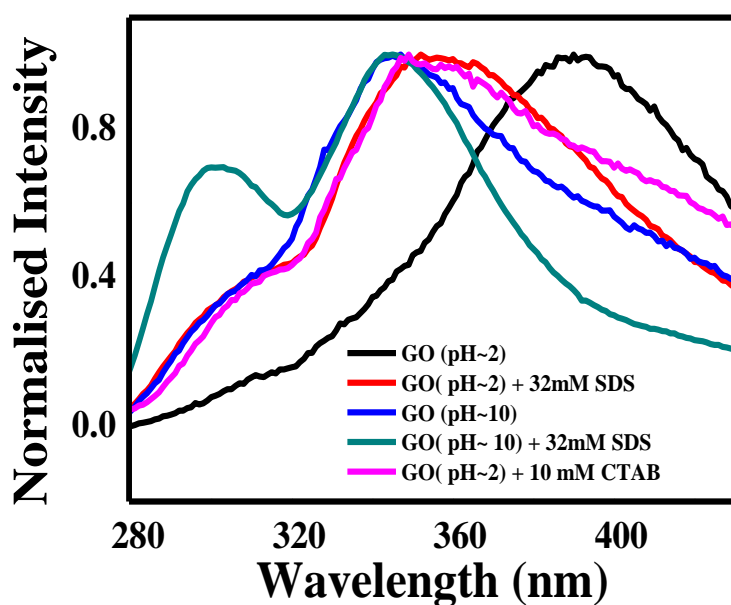


Fig. 7 Normalized photoluminescence spectra of aqueous dispersion of GO (pH \approx 2), aqueous dispersion of GO (pH \approx 2) and 32 mM SDS, aqueous dispersion of GO (pH \approx 10), aqueous dispersion of GO (pH \approx 10) and 32 mM SDS, aqueous dispersion of GO (pH \approx 2) and 10 mM CTAB

The blue shift of emission maxima of GO in the acidic medium is obtained in two stages in the presence of SDS. This two stage blue shift in the presence of SDS may be due to the nonpolar environment around the fluorophoric moiety, resulting from the adsorption of SDS on GO surface. Above 2 mM concentration of SDS, monolayer adsorption of SDS on the GO sheets has been taken place and our photoluminescence study confirms that critical surface aggregation constant (CSAC) is greater than 2 mM which is very close to the observation of Hsieh et al. [9,10]. Above 12 mM SDS concentration, hemi spherical surface micelles are formed on the GO surface resulting a highly non polar environment around the fluorophoric moiety. Whereas, the blue shift of emission maxima of GO in the acidic medium is obtained in one stage in the presence of CTAB of concentration of equal or above 2mM, which is due to creation nonpolar environment by forming hemispherical surface micelle. Again, the carboxylic functional groups of GO are negatively charged in alkaline medium (pH \approx 10), repulsion between these negatively charged carboxylate groups increases the interlayer spacing of GO and this leads to a blue shift in emission maxima [30]. In the presence of SDS, the interlayer spacing of GO (pH~10) becomes very high due to very weak π - π stacking interaction because of the intercalation of SDS molecules between successive GO sheets, and this may give rise to largely separated layers of the GO moiety with almost isolated benzoic acid or phenol like species resulting the increase in the intensity of the photoluminescence band at 303 nm (Fig. 8b). The low intense luminescence band at 305 nm also appeared in acidic medium of GO in the presence both CTAB and SDS, which is due to very weak π - π interaction by the intercalation of surfactants between GO layers.

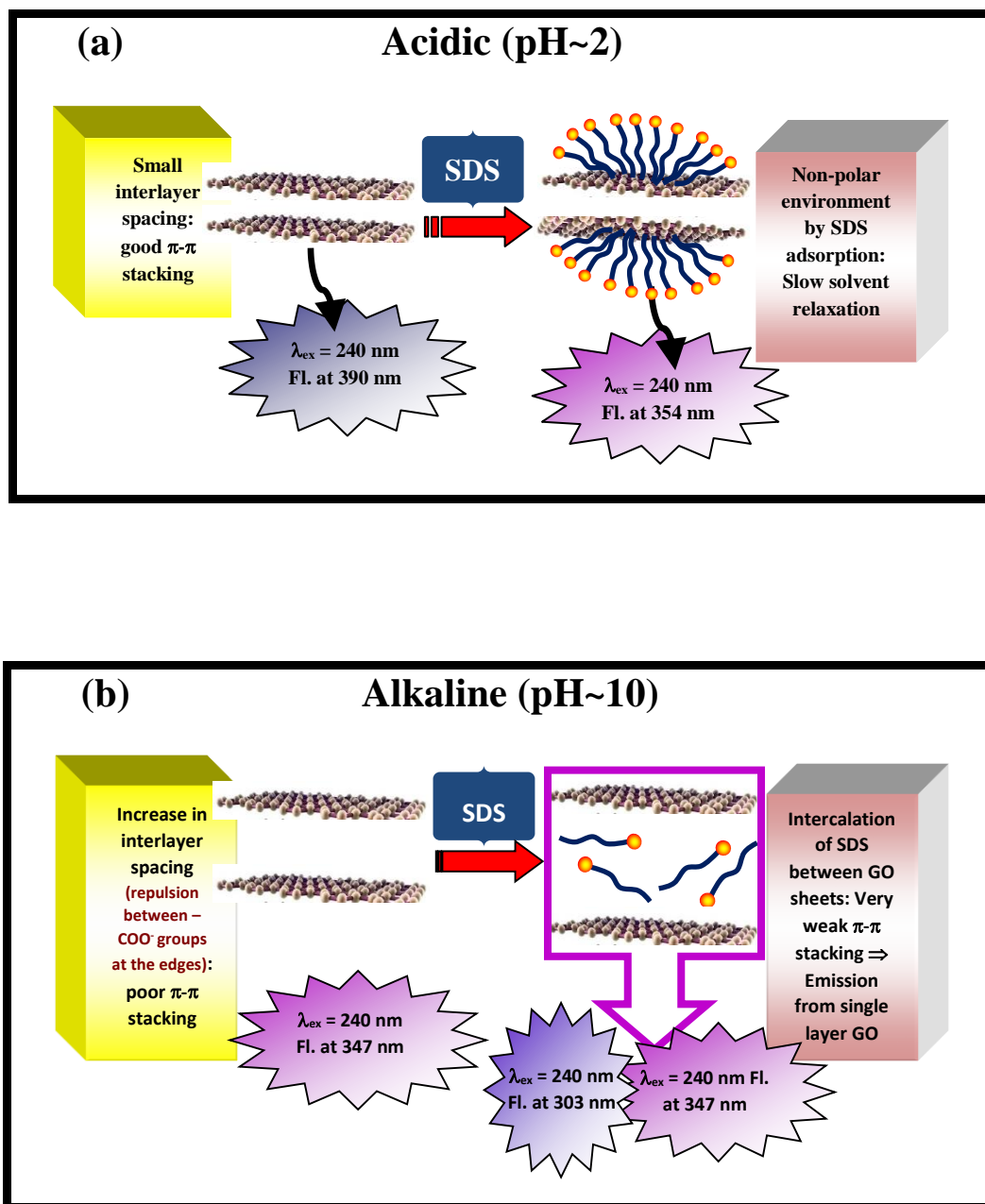


Fig. 8 Schematic diagram representing the interlayer spacing between GO sheets and effect of SDS on the emission at (a) acidic (pH \approx 2) (b) alkaline (pH \approx 10)

5.3.5. Fluorescence Excitation Spectra of GO

We have measured the fluorescence excitation spectra (FLE) of aqueous dispersion GO at $\text{pH} \approx 2$ in presence and absence of SDS (Fig. 9a and 9b). The FLE also measured from aqueous dispersion GO at $\text{pH} \approx 2$ in presence and absence of CTAB (Fig. 10a and 10b). Fluorescence excitation spectra (FLE) of GO in acidic medium ($\text{pH} \approx 2$) monitored at 390 nm (Fig. 9a and Fig. 10a) shows a major band at 240 nm for both presence and absence of SDS and CTAB respectively. This suggests that the species emitting at 390 nm absorbs at 240 nm [30] and adsorption of SDS and CTAB on GO surface does not create any new fluorophoric species. But, FLE monitored at 350 nm for the aqueous dispersion of GO ($\text{pH} \approx 2$) in the presence of 32 mM SDS (Fig. 9b) and 10mM CTAB (Fig. 10b) shows two distinct bands at 230 nm and 280 nm. But, the very low intensity of FLE band monitored at 350 nm for acidic dispersion of only GO is suggesting the very low contribution of the species giving fluorescence at 350 nm.

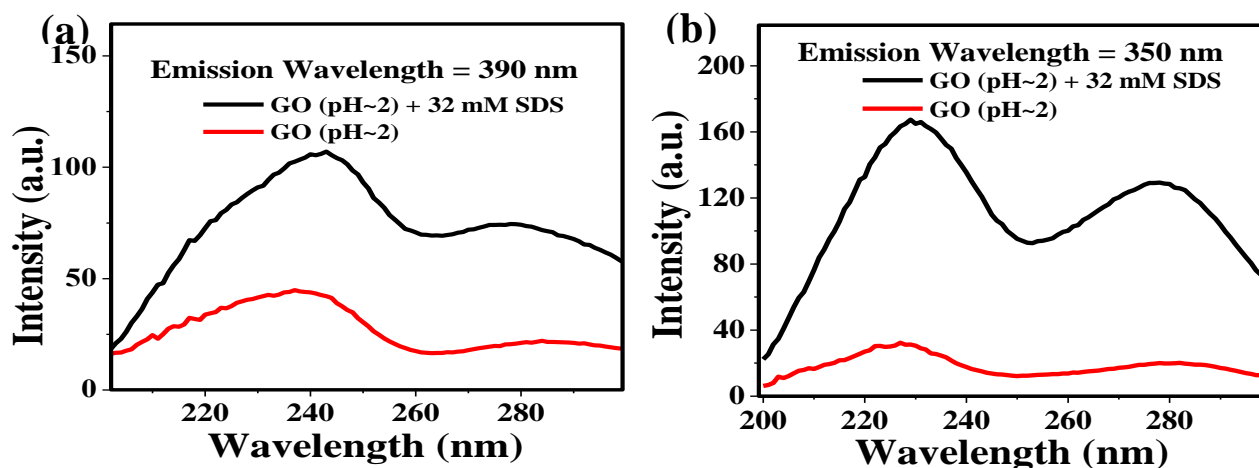


Fig. 9 Excitation Spectra of GO Dispersion ($\text{pH} \approx 2$) in presence and absence of SDS

(a) $\lambda_{\text{em}} = 390 \text{ nm}$ (b) $\lambda_{\text{em}} = 350$

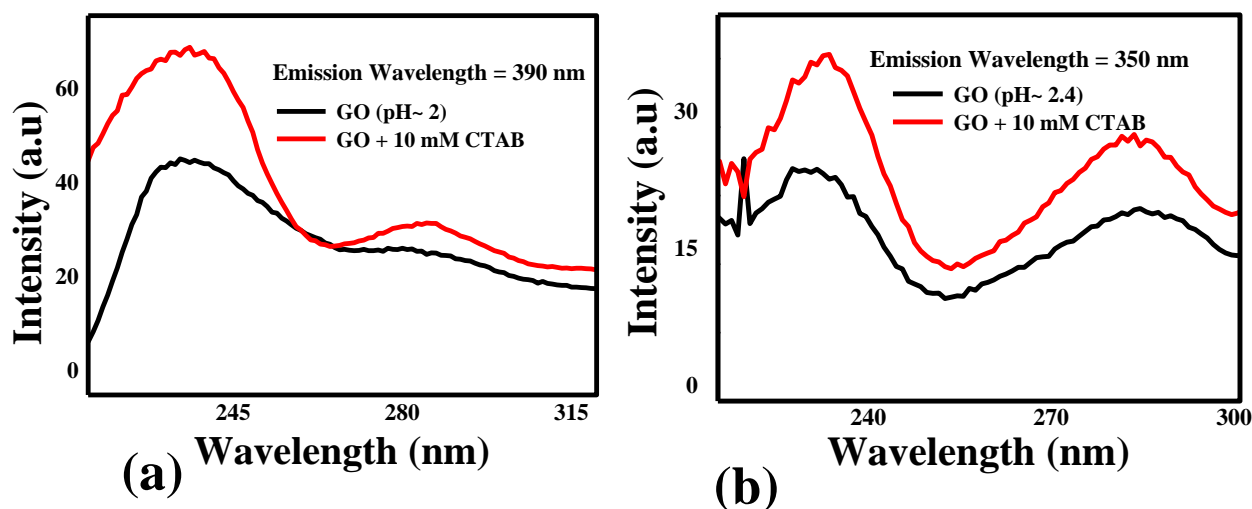


Fig. 10 Excitation Spectra of GO Dispersion (pH \approx 2) in presence and absence of CTAB

(a) $\lambda_{em} = 390$ nm (b) $\lambda_{em} = 350$ nm

In this context, it can be mentioned that the observed FLE bands at 280 nm and 230 nm resembles to first and second singlet-singlet transition in benzoic acid, respectively [31]. Since the chemically functionalized GO contain carboxylic groups attached with the hexagonal sp^2 hybridized carbon atoms, the presence of FLE band at 280 nm and 230 nm is quite natural. FLE spectra, monitored at 303 nm and 347 nm, (Fig. 11a and 11b) in the alkaline medium (pH \approx 10) remain identical in the presence and absence of SDS and this suggests fluorophoric moieties in the excited states are originated from same ground state species. Excitation emission matrices (EEM) of GO dispersion in alkaline pH (Fig. 11c) provide an important observation regarding the photoluminescence band at 303 nm. EEMs clearly indicates that the emission centered at 303 nm is obtained by the excitation at π - π^* band (220 – 230 nm) as well as n - π^* band (270 – 290 nm) and the intensity of photoluminescence at 303 nm gradually increases with the increase in SDS concentration. From this observation, one may conclude that with increase in the extent of SDS intercalation, the distance between the successive layers of GO increases.

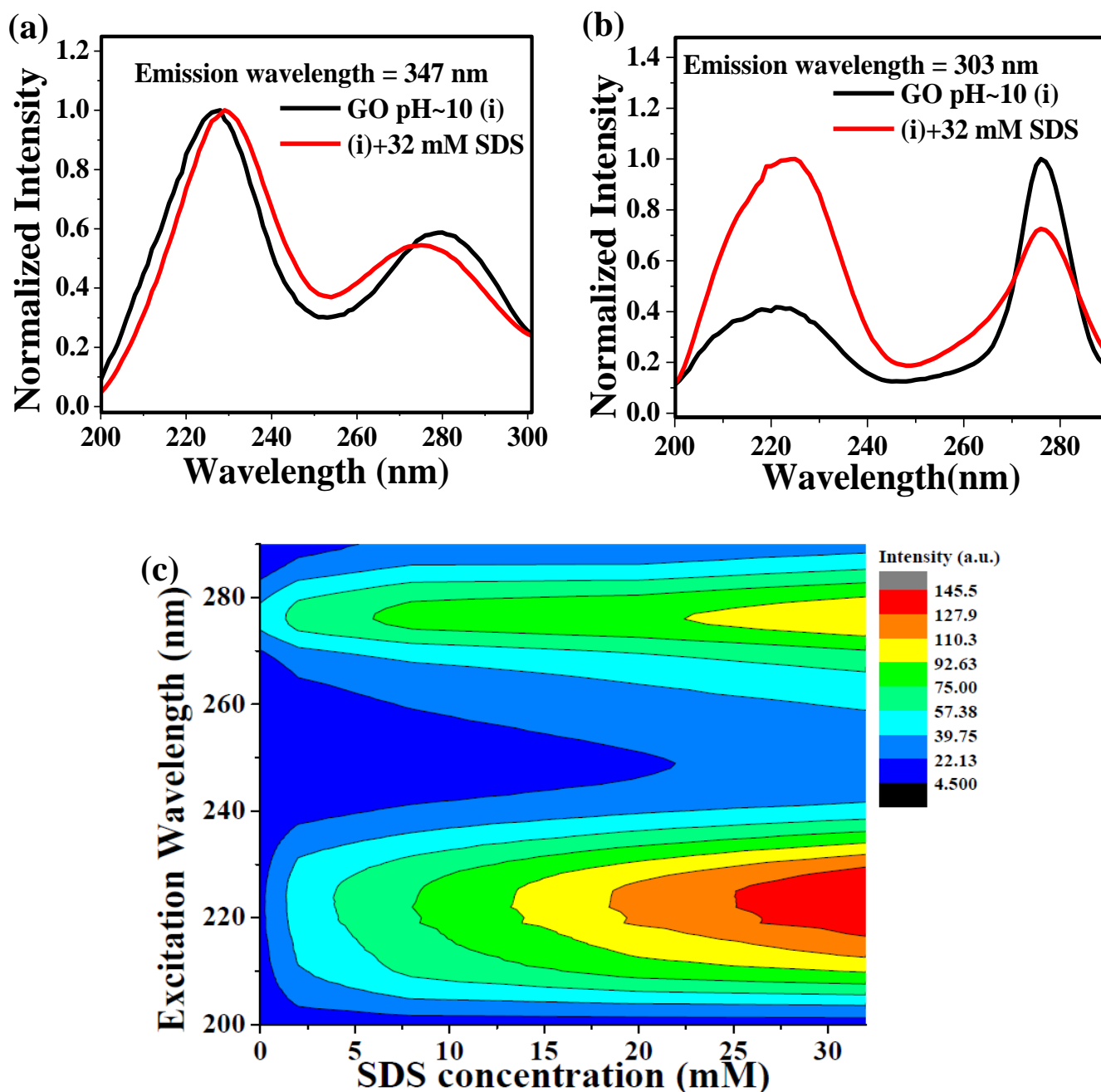


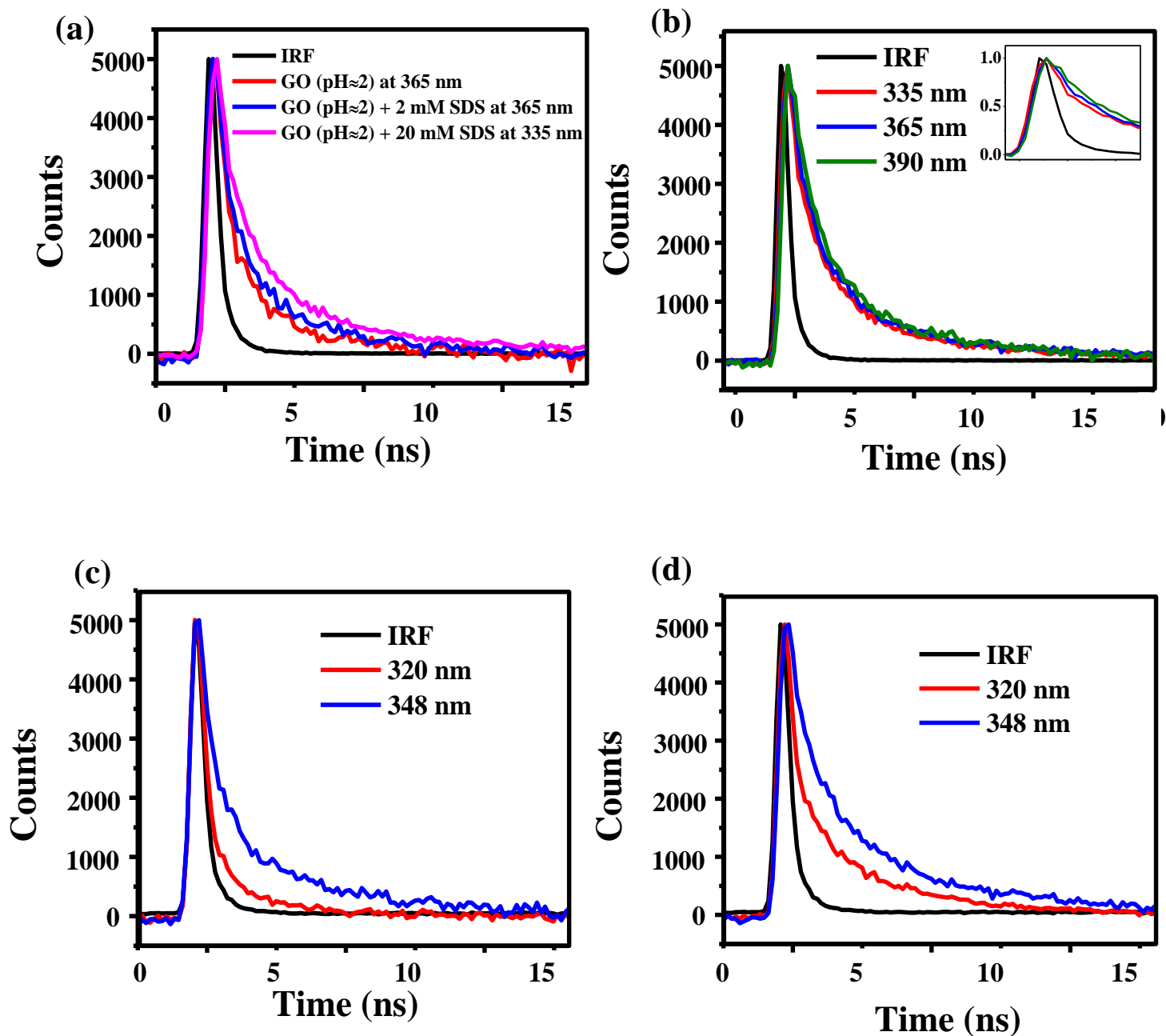
Fig. 11 Excitation Spectra of GO Dispersion (pH ≈ 10) in presence and absence of SDS

(a) $\lambda_{em} = 347$ nm (b) $\lambda_{em} = 303$ nm (c) Excitation-Emission Matrix of GO (pH ≈ 10) for different SDS concentration (monitored at 303 nm)

Fig. 12a indicates that the fluorescence decays at 365 nm obtained by exciting the aqueous GO dispersion ($\text{pH} \approx 2$) in absence and presence of 2 mM SDS by exciting at 280 nm are almost same and bi-exponential with average life time of about 1000 ps (Table 1). But, addition of more SDS results a blue shift in emission maxima and finally, in the presence of 20 mM SDS, the fluorescence maxima is shifted to 333 nm (Fig. 2b). The average life time obtained at 335 nm for acidic dispersion of GO ($\text{pH} \approx 2$) in the presence of 20 mM SDS was found to be about 1.9 times higher than the average life time of aqueous dispersion of GO in absence of SDS (Table 1). The increase in the life time may be interpreted by the decrease in the non-radiative pathways may be due to the decrease in the accessibility of polar solvent molecules around the fluorophoric moiety of GO. The formation of hemispherical SDS micelles on the GO sheets [9] introduces a confinement to the motion of water molecules at the surface of GO and there by slow down the relaxation process of the GO fluorophore in the excited state. The restricted motion of the solvent molecules surroundings the GO fluorophore results time dependent fluorescence stokes shift which is usually manifested by wavelength dependent fluorescence decays. But, the time resolution of our instrument (instrument response function ≈ 600 ps) is not high enough to detect such kinds of fluorescence decays and a distinct growth of the fluorescence decay obtained at the red end of the emission band. The fluorescence decays of aqueous dispersion of GO in presence of 20 mM SDS at 335 nm, 365 nm and 390 nm are not well separated (Fig. 12b). But, Table 2 shows that the magnitude of the slow components of the fluorescence decays increase from 3.6 to 5.9 ns with the increase in wavelength may be due to the slow solvent relaxation.

In the alkaline medium ($\text{pH} \approx 10$), aqueous dispersion of GO shows two emission bands at 303 nm and 347 nm in presence of SDS (Fig. 6a). The existence of dual peaks is already explained by weakening of π - π stacking interaction between successive GO layers

Fig. 12



(a) Fluorescence decays at emission maxima of aqueous dispersion of GO ($\text{pH} \approx 2$) in presence and absence of SDS (b) Fluorescence decays at different wavelengths of aqueous dispersion of GO ($\text{pH} \approx 2$) in presence of 20 mM SDS (c) Fluorescence decays at 320 nm and 350 nm of aqueous dispersion of GO ($\text{pH} \approx 10$) (d) Fluorescence decays at 320 nm and 350 nm of aqueous dispersion of GO ($\text{pH} \approx 10$) and 32 mM SDS ($\lambda_{ex} = 280$ nm)

due to the intercalation of SDS within the GO sheets and the PL bands of benzoic acid or phenol like moiety. Observation of such dual peaks due to any kind of excited state phenomenon can be studied by time resolved fluorescence. Since, the excitation wavelength of our TCSPC set up is 280 nm, we have measured the fluorescence decays of alkaline dispersion of GO in presence and absence of SDS at 348 nm and 320 nm (instead of 303 nm) to avoid any interference from Raman scattering. The fluorescence decays at two wavelengths 348 nm and 320 nm are distinct in nature both in the presence and absence of SDS and fitted well by a bi-exponential decay function (Fig 12c and Fig. 12d). The fast decay process (τ_1) with a lifetime shorter than 1000 ps is due to non-radiative re-combination process, while the slow decay process (τ_2) originates from the radiative decay [40]. The lifetime of radiative component of the slow decay process at 320 nm is 3-3.5 ns and while at 348 nm, it is 4.7-5.2 ns. The relative contribution of the radiative component of the slow decay process at 320 nm is found to be increased about 6 times with the increase in concentration of SDS (Table 3). As, the low wavelength band at 303 nm is obtained due to well separated layers of GO moiety consists of benzoic acid or phenol like structure as a result of disruption of π - π stacking interaction by intercalation of SDS molecules, the increase in relative contribution of this decay component (3-3.5 ns) is due to increase in the extent of SDS intercalation within GO layers. Again, in the acidic medium (pH \approx 2), similarities of the decay parameters of GO dispersion in the presence of 20 mM SDS at 320 nm (Table 2) indicates the adsorption of SDS in the form of hemispherical micelles as well as intercalation of SDS within the GO sheets resulting the increase in the distance between the GO layers. The longer life time of the slow component at 348 nm compared to the slow component at 320 nm may be explained by the symmetry argument. Du et al mentioned that the origin of the longer life time is related to the symmetry of the electronic states of excimer wave function [38]. According to Conwell et al, the similar parities of the ground state monomer and excimer is responsible for such longer life time [41].

Fluorescence decay of GO (pH~2) in the presence of CTAB not studied within this time period and need to study for confirmation and future reference.

Table 1

**Fluorescence decay parameters of aqueous GO dispersion (pH \approx 2)
in presence and absence of SDS at emission maxima ($\lambda_{\text{ex}} = 280$ nm)**

Conc. of SDS (mM)	Wavelength (nm)	τ_1^a	τ_2^a	$\langle \tau \rangle$
0	365	670 ps (94%)	4.2 ns (6%)	880 ps
2	365	600 ps (87%)	4.4 ns (13%)	1090 ps
20	335	1000 ps (82%)	4.8 ns (18%)	1680 ps

a \pm 10 %

Table 2

**Fluorescence decay parameters of aqueous GO dispersion (pH \approx 2)
in presence of 20 mM SDS at different wavelengths ($\lambda_{\text{ex}} = 280$ nm)**

Wavelength (nm)	τ_1^a	τ_2^a
320	900 ps (82%)	3.6 ns (18%)
335	1000 ps (82%)	4.8 ns (18%)
365	1000 ps (82%)	5.5 ns (18%)
390	1000 ps (80%)	5.9 ns (20%)

a \pm 10 %

Table 3

**Fluorescence decay parameters of aqueous GO dispersion (pH \approx 10)
in presence and absence of SDS ($\lambda_{\text{ex}} = 280$ nm)**

SDS concentration	Fluorescence lifetime at 320 nm		Fluorescence lifetime at 348 nm	
	τ_1^a	τ_2^a	τ_1^a	τ_2^a
0 mM	300 ps (96%)	3.0 ns (4%)	500 ps (85%)	4.7 ns (15%)
4 mM	500 ps (90%)	3.0 ns (10%)	600 ps (88%)	4.8 ns (12%)
12 mM	550 ps (83%)	3.1 ns (17%)	800 ps (85%)	5.1 ns (15%)
20 mM	750 ps (75%)	3.5 ns (25%)	1000 ps (73%)	5.2 ns (27%)

$a \pm 10 \%$

The life time (τ^a) can be reproduced within $\pm 10 \%$ uncertainty

5.4. Conclusion

The present work demonstrates the change in luminescence of GO as a result of interaction between an anionic surfactant (SDS) and a cationic surfactant CTAB in both acidic and alkaline medium. In the acidic medium (pH \approx 2) of GO, the surfactant, SDS, is adsorbed on the GO sheets and the critical surfactant aggregation constant (CSAC) is obtained at a SDS concentration greater than 2 mM. Adsorption of SDS on the GO sheets as hemispherical micelles, at pH \approx 2 modulates the photoluminescence band by providing a nonpolar confined environment. The blue shift of emission maxima of GO in the acidic medium in the presence of CTAB may also due to the creation of nonpolar environment by the formation of hemispherical surface micelle. As a result of this, the acidic dispersion of GO in presence of 32 mM SDS shows red edge effects which is a common consequence of restricted solvent

relaxation process. Observation of the increase in the fluorescence life time of the fluorophoric moiety of GO with increase in SDS concentration is suggesting the decrease in nonradiative decay process due to lower accessibility of solvent molecules near the GO fluorophores. In the alkaline medium, instead of adsorption on GO sheets, intercalation of SDS molecules within the GO layers may occur and these intercalations enhance the distance between successive GO sheets. This leads to the weakening of π - π stacking interaction between the basal planes of GO. The time resolved photoluminescence data also supports the entire scenario and indicate the presence of two types of GO moieties, one with weak π - π stacking interaction another with almost disrupted π - π interaction between GO sheets containing benzoic acid or phenol like structure due to the intercalation of SDS, results dual photoluminescence band in alkaline medium. The entire work shades light on the interesting photoluminescence features and modulation of photoluminescence spectra of GO by the surfactants (SDS, CTAB) and thereby will help to develop various kinds of GO based optoelectronic materials.

5.5. Reference

- [1] D. A. Dikin, S. Stankovich, E. J. Zimney, R. D. Piner, G. H. B. Dommett, G. Evmenenko, S. T. Nguyen and R. S. Ruoff, *Nature*, 2007, **448**, 457- 460.
- [2] T. Szabó, O. Berkesi, P. Forgo, K. Josepovits, Y. Sanakis, D. Petridis and I. Dekany, *Chem. Mater.*, 2006, **18(11)**, 2740–2749.
- [3] H. B. Lee, A. V. Raghu, K. S. Yoon and H. M. Jeong, *J. Macromol. Sci. Phys.*, 2010, **49**, 802–809.
- [4] J. Wang, X. Wang, C. Xu, M. Zhang and X. Shang, *Polym. Int.*, 2011, **60**, 816–822.
- [5] C. Bao, Y. Guo, L. Song and Y. Hu, *J. Mater.Chem.*, 2011, **21**, 13942–13950.
- [6] N. W. Pu, C. A. Wang, Y. M. Liu, Y. Sung, D. S. Wang and M. D. Ger, *J. Taiwan Inst. Chem. Eng.*, 2012, **43**, 140–146.
- [7] K. Zhang, L. Mao, L. L. Zhang, H. S. O. Chan, X. S. Zhao and J. Wu, *J. Mater. Chem.*, 2011, **21**, 7302-7307.
- [8] A.J. Glover, D. H. Adamson and H. C. Schniepp, *J. Phys. Chem.C*, 2012, **116**, 20080–20085.
- [9] A. G. Hsieh, C. Punckt, S. Korkut and I. A. Aksay, *J. Phys. Chem. B*, 2013, **117**, 7950–7958.
- [10] A. G. Hsieh, S. Korkut, C. Punckt and I. A. Aksay, *Langmuir*, 2013, **29(48)**, 14831–14838.
- [11] D. Wang, D. Choi, J. Li, Z. Yang, Z. Nie, R. Kou, D. Hu, C. Wang, L.V. Saraf, J. Zhang, I. A. Aksay and J. Liu, *ACS Nano*, 2009, **3**, 907–914.
- [12] D. Wang, R. Kou, D. Choi, Z. Yang, Z. Nie, J. Li, L.V. Saraf, D. Hu, J. Zhang, G. L. Graff, J. Liu, M. A. Pope and I. A. Aksay, *ACS Nano*, 2010, **4**, 1587–1595.
- [13] I. A. Aksay, M. Trau, S. Manne, I. Honma, N. Yao, L. Zhou, P. Fenter, P. M. Eisenberger and S. M. Gruner, *Science*, 1996, **273**, 892–898.

- [14] K. S. Choi, H. C. Lichtenegger, G. D. Stucky and E. W. McFarland, *J. Am. Chem. Soc.*, 2002 **124**, 12402–12403.
- [15] D. Yang, A. Velamakani, G. Bozoklu, S. Park, M. Stoller, R. D. Piner, S. Stankovich, I. Jung, D. A. Field, C. A. Ventrice and R. S. Ruoff, *Carbon*, 2009, **47**, 145-152.
- [16] B. Konkena and S. Vasudevan, *J. Phys. Chem. Lett.*, 2012, **3**, 86–872.
- [17] D. Li, M. B. Mulle, S. Gilje, R. B. Kaner and G. G. Wallace, *Nat. Nanotechnol.*, 2008, **3**, 101-105.
- [18] Z. Kiraly, G. Findenegg, E. Klumpp, H. Schlimper and I. Dekany, *Langmuir*, 2001, **17**, 2420–2425
- [19] N. R. Tummala, B. P. Grady and A. Striolo, *Phys. Chem. Chem. Phys.*, 2010, **12**, 13137–13143.
- [20] M. Sammalkorpi, A. Z. Panagiotopoulos and M. Haataja, *J. Phys. Chem. B*, 2008, **112**, 12954–12961.
- [21] P. Dutta, J. Afalla, A. Halder, S. Datta and K. Tominaga, *J. Phys. Chem. C*, 2017, **121**, 1442-1448.
- [22] W. Meng, E. Gall, F. Ke, Z. Zeng, B. Kopchick, R. Timsina, X.. Qiu, *J. Phys. Chem. C* 2015, **119**, 21135 –21140
- [23] E. Vaghri, D. Dorranean, M. Ghoranneviss *Materials Chemistry and Physics*, 2018, **203**, 235- 242.
- [24] A. Ganguly, S. Sharma, P. Papakonstantinou, J. Hamilton, *The Journal of Physical Chemistry C*, 2011, **115**, 17009–17019.
- [25] S.J. Wang, Y. Geng, Q. Zheng, J.-K. Kim, *Carbon*, 2010, **48**, 1815–1823.
- [26] S. Bykkam, V. K. Rao, S. CH. Chakra, T. Thunugunta, *Int. J. Adv. Biotech. and Research* 2013 **4** 142-146.
- [27] S. N. Alam, N. Sharma, L. Kumar, *Scientific Research Publishing*, 2017, **6**, 1-18.

- [28] Z. Luo, Y. Lu, L. A. Somers and A. T. C. Johnson, *J. Am. Chem. Soc.*, 2009, **131**, 898-899.
- [29] B. J. Clark, T. Frost and M. A. Russell, *UV Spectroscopy: Techniques, Instrumentation, Data Handling/UV Spectrometry Group*, Chapman & Hall:London, New York, 1993, **4**.
- [30] P. Dutta, D. Nandi, S. Datta, S. Chakraborty, N. Das, S. Chatterjee, U. C. Ghosh and A. Halder, *J. of Lumin.*, 2015, **168**, 269–275.
- [31] H. Hosoya, J. Tanaka and S. Nagakura, *J. Mol. Spectrosc.*, 1962, **8**, 257- 275.
- [32] L. Reynold, J. A. Gardecki, S. J. Frankland, M. L. Hong and M. Marocelli, *J. Phys. Chem.*, 1996, **100**, 10337-10354.
- [33] S. K. Cushing, M. Li, F. Huang and N. Wu, *ACS Nano*, 2014, **8**, 1002–1013.
- [34] M. Li, S. K. Cushing, X. Zhou, S. Guo and N. Wu, *J. Mater. Chem.*, 2012, **22**, 23374.
- [35] D. Kozawa, Y. Miyauchi, S. Mouri and K. Matsuda, *J. Phys. Chem. Lett.*, 2013, **4**, 2035-40.
- [36] I. B. Berlman, *Handbook of florescence spectra of Aromatic Molecules*, 2nd Rev.ed. Academic Press, New York, 1971.
- [37] Y. Song, H. Lee, J. Ko, J. Ryu, M. Kim and D. Shon, *Bull. Korean Chem. Soc.*, 2014, **35**, 2009 – 2012.
- [38] D. Du, H. Song, Y. Nie, X. Sun, L. Chen and J. Ouyang, *J. Phys. Chem.C*, 2015, **119**, 20085-20090
- [39] W. T. Yip, D. H. Levy and *J. Phys. Chem.*, 1996, **100(28)**, 11539–11545.
- [40] C. Jagadish and S. J. Pearton, *Zinc Oxide Thin Films and Nanostructures Processing Properties and Application*, Elsevier Science: Amsterdam, 2011.
- [41] E. Conwell, *Phys Rev. B: Condens Mater Phys.*, 1998, **57**, 14200-14202.